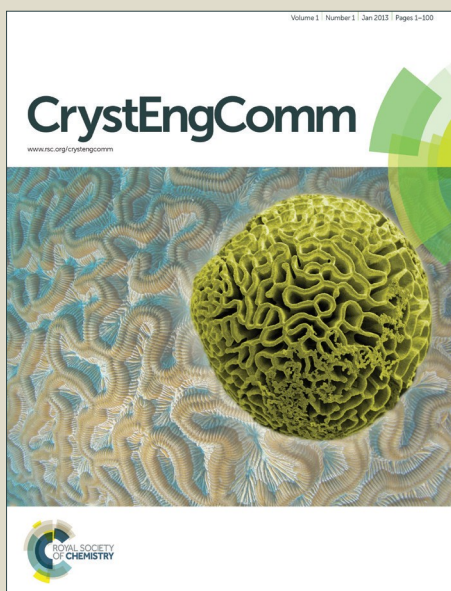


CrystEngComm

Accepted Manuscript



This is an *Accepted Manuscript*, which has been through the Royal Society of Chemistry peer review process and has been accepted for publication.

Accepted Manuscripts are published online shortly after acceptance, before technical editing, formatting and proof reading. Using this free service, authors can make their results available to the community, in citable form, before we publish the edited article. We will replace this *Accepted Manuscript* with the edited and formatted *Advance Article* as soon as it is available.

You can find more information about *Accepted Manuscripts* in the [Information for Authors](#).

Please note that technical editing may introduce minor changes to the text and/or graphics, which may alter content. The journal's standard [Terms & Conditions](#) and the [Ethical guidelines](#) still apply. In no event shall the Royal Society of Chemistry be held responsible for any errors or omissions in this *Accepted Manuscript* or any consequences arising from the use of any information it contains.



Journal Name

COMMUNICATION

A single-crystal to single-crystal phase transition in $[\text{Co}(\text{NH}_3)_5\text{NO}_2]\text{Br}_2$ at high pressure: a step towards understanding linkage photo-isomerisation

Received 00th January 20xx,
Accepted 00th January 20xx

DOI: 10.1039/x0xx00000x

B. A. Zakharov,^{a,b} A. S. Marchuk^{b,a} and E. V. Boldyreva^{b,a}

www.rsc.org/

Changes in the crystal structure of $[\text{Co}(\text{NH}_3)_5\text{NO}_2]\text{Br}_2$ - including a previously unknown single-crystal to single-crystal phase transition above 6.0 GPa - were followed from ambient pressure to 6.9 GPa and discussed in relation to the structural mechanism of homogeneous linkage photoisomerisation that is accompanied by photomechanical effects in the same compound.

Introduction

Solid-state chemical reactions are accompanied by the generation and relaxation of mechanical stresses and strain. These phenomena are of utmost importance for the reaction kinetics and spatial propagation^{1–3}. Homogeneous single-crystal to single-crystal reactions are of special interest as they make it possible to follow structural strain by single-crystal X-ray diffraction. Some of these reactions are accompanied by various photo- and thermomechanical effects, including bending, twisting, curling, jumping of crystals, amongst others³. One of the first examples for which photomechanical effects were documented – and extensively studied in the 1980s – was a series of Co(III) coordination compounds with the general formula $[\text{Co}(\text{NH}_3)_5\text{NO}_2]\text{XY}$ (where X, Y = Br, Cl, I, NO_3)^{2,4–6}. Over the past decade, interest in this system was revived⁷. Within this family of compounds the coordination of the nitro ligand changes on irradiation, linking to cobalt *via* the oxygen rather than the nitrogen atom, $[\text{Co}(\text{NH}_3)_5\text{NO}_2]\text{XY} \rightarrow [\text{Co}(\text{NH}_3)_5\text{ONO}]\text{XY}$. This reaction is accompanied by significant anisotropic strain. $[\text{Co}(\text{NH}_3)_5\text{NO}_2]\text{Br}_2$ is the only compound for which the structure of the nitrito-isomer, which is formed on irradiation, has been solved (from powder diffraction data)⁸. The structural mechanisms of photochemical reactions in

crystals are closely related to the anisotropy of mechanical properties, which can be followed particularly well by studying the crystal structure under pressure^{5,7–10}. For example, the mechanism of the photosensitive effect⁷ and the effect of elastic loading on the quantum yield of the photoisomerisation in $[\text{Co}(\text{NH}_3)_5\text{NO}_2]\text{Cl}(\text{NO}_3)$ ^{12,13} could be rationalised by comparing lattice strain on isomerisation¹⁴ with structural distortion induced by increasing pressure¹¹.

For $[\text{Co}(\text{NH}_3)_5\text{NO}_2]\text{Br}_2$, only pressure-dependence of cell parameters has been reported based on a powder diffraction study, 4 GPa being the highest pressure point reached to date¹¹. The aim of the present work was to follow in detail the structural changes in $[\text{Co}(\text{NH}_3)_5\text{NO}_2]\text{Br}_2$ on increasing hydrostatic pressure by single-crystal diffraction. This work sought to correlate these results with data on the structural distortion over the course of photo-induced nitro-nitrito isomerisation in the same compound.

Crystallisation of the target compound was performed in the following way. $[\text{Co}(\text{NH}_3)_5\text{NO}_2](\text{NO}_3)_2$ powder (3.22 g) was dissolved in water (105 ml) and heated to ~75 °C. NH_4Br (7.45 g) was subsequently added to the solution and crystallisation of $[\text{Co}(\text{NH}_3)_5\text{NO}_2]\text{Br}_2$ was observed. After stirring and cooling for 30 min to ambient temperature, the precipitate was filtered off and rinsed with ethanol. The target compound was recrystallised from aqueous solution by slow evaporation over a period of one week.

Pressure was generated using a Boehler-Almax¹⁵ diamond anvil cell (DAC). A stainless steel gasket with initial thickness of 200 μm was pre-indented to ~100 μm . A hole of 300 μm in diameter was drilled in the gasket using the spark erosion technique. A single crystal of $[\text{Co}(\text{NH}_3)_5\text{NO}_2]\text{Br}_2$ (0.20 x 0.20 x 0.05 mm) was loaded in the DAC with a methanol-ethanol (4:1) mixture as hydrostatic medium^{16,17}. The ruby fluorescence line was used for pressure calibration with an accuracy of $\pm 0.05 \text{ GPa}$ ¹⁸.

^a Institute of Solid State Chemistry and Mechanochemistry SB RAS, 630128, Kutateladze Street 18, Novosibirsk, Russian Federation. E-mail: b.zakharov@yahoo.com.

^b Novosibirsk State University, 630090, Pirogova Street 2, Novosibirsk, Russian Federation.

† Electronic Supplementary Information (ESI) available: table of crystal structure refinement parameters (Table 1), movie showing crystal structure changes on phase transition (M1), CIFs and structure factor files, CheckCIF report. See DOI: 10.1039/x0xx00000x

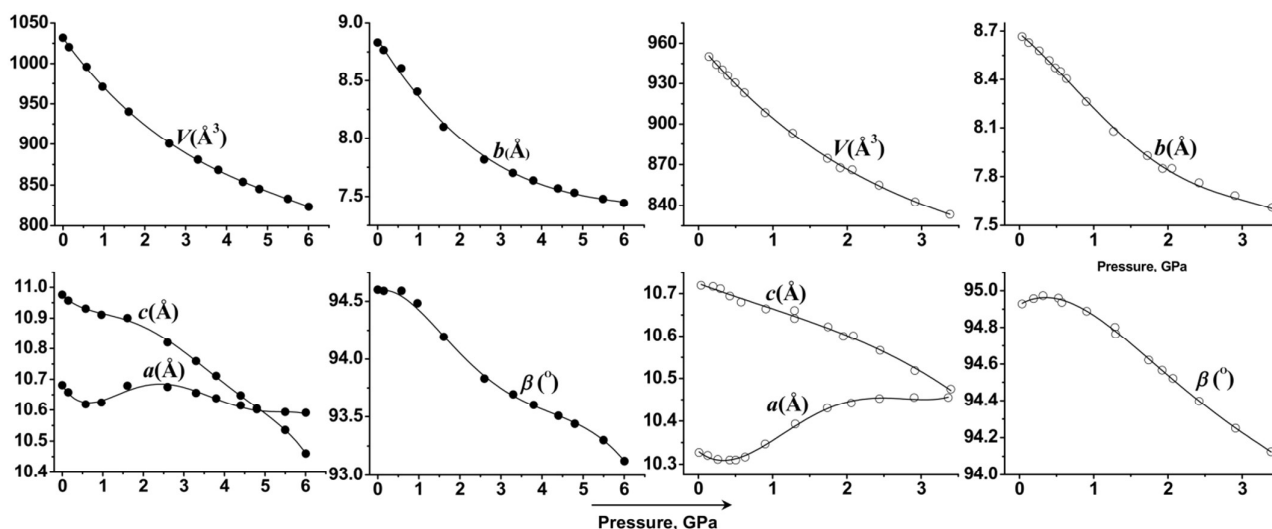


Figure 1. Cell parameters for $[\text{Co}(\text{NH}_3)_5\text{NO}_2]\text{Br}_2$ at different pressures measured in this work below the phase transition point (black symbols), and selected points for $[\text{Co}(\text{NH}_3)_5\text{NO}_2]\text{Cl}_2$ taken from Ref⁹ (open symbols).

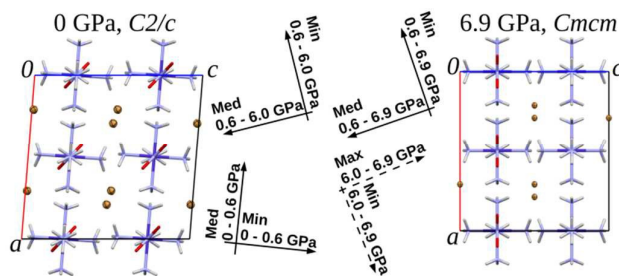


Figure 2. Directions of the strain ellipsoid principal axes for $[\text{Co}(\text{NH}_3)_5\text{NO}_2]\text{Br}_2$ at different pressures. Dashed arrows show deformations corresponding to the structural transition. Rotation of the NO_2 group occurs counterclockwise.

Diffraction data sets were collected using an Oxford Diffraction Gemini R Ultra X-ray diffractometer with Mo- $\text{K}\alpha$ radiation and a CCD area detector. Data were collected between ambient pressure and 6.9 GPa. Data collection, cell determination and data integration were performed using the CrysAlisPro software¹⁹. Sample reflections overlapping with the diamond and gasket reflections were manually excluded. Gaussian absorption correction was performed using Absorb-7 with Absorb-GUI²⁰. The initial crystal structure model for structure refinement up to 6.0 GPa was taken from Ref²¹. Refinement was carried out with SHELXL2014²² using X-Step 32²³ as the GUI. Hydrogen atom parameters were constrained using the AFIX 33 instruction (riding model) with $\text{Uiso}(\text{H}) = 1.5\text{Ueq}(\text{N})$, $\text{N}-\text{H} = 0.89 \text{ \AA}$ for NH_3 -groups. Atomic parameters were refined anisotropically without any restraints. Deformation along the strain ellipsoid principal axes were calculated using the Win_Strain software²⁴. The crystal structure of the high-pressure phase was solved by direct methods implemented in the SIR2004 software²⁵ and refined in the same way as the monoclinic structure at lower pressures. Although the single

crystal was preserved after the transformation, atomic displacement parameters for the high-pressure phase were not satisfactory and DELU (rigid-bond) and SIMU (similar-ADP) SHELX restraints with default values were used to bring them to reasonable values. Mercury²⁶, Platon²⁷ and enCIFer²⁸ were used for structure visualisation, analysis and preparing the CIF for publication. Data collection and refinement parameters, as well as crystal data are summarised in ESI, Table S1. Complete structural data were deposited in the CSD²⁹ with refcodes CCDC 1423454-1423466.

The structural model for $[\text{Co}(\text{NH}_3)_5\text{NO}_2]\text{Br}_2$ at ambient conditions agreed well with previously published data^{21,30}. From ambient pressure to 6.0 GPa the crystal structure of $[\text{Co}(\text{NH}_3)_5\text{NO}_2]\text{Br}_2$ compressed anisotropically. The pressure-dependence of cell parameters and volume agreed with those previously reported below 4 GPa¹¹ (Figure 1). This work extends previous reports, having determined for the first time the pressure-dependence of cell parameters and volume above 4 GPa, as well as the atomic coordinates at multiple points across the pressure range 1 atm – 6.9 GPa. The directions of the strain ellipsoid principal axes are shown in relation to the fragments of the crystal structure in Figure 2. The direction of the minimum and medium compression in the ac plane interchanged at 0.6 GPa (Figure 2). Strain in this plane was mostly caused by slight rotation of the $-\text{NO}_2$ group (see animation M1 in ESI). Maximum compression was observed along the crystallographic b axis, coinciding with the direction of the $\text{Co}-\text{NO}_2$ bond. This can be related to filling void space in the crystal structure between the $-\text{NO}_2$ and $-\text{trans}-\text{NH}_3$ ligands at pressures below 6.0 GPa. On further increasing pressure, the structure could not be compressed anymore in this direction without a significant rotation of the $-\text{NO}_2$ group (see discussion of the phase transition below).

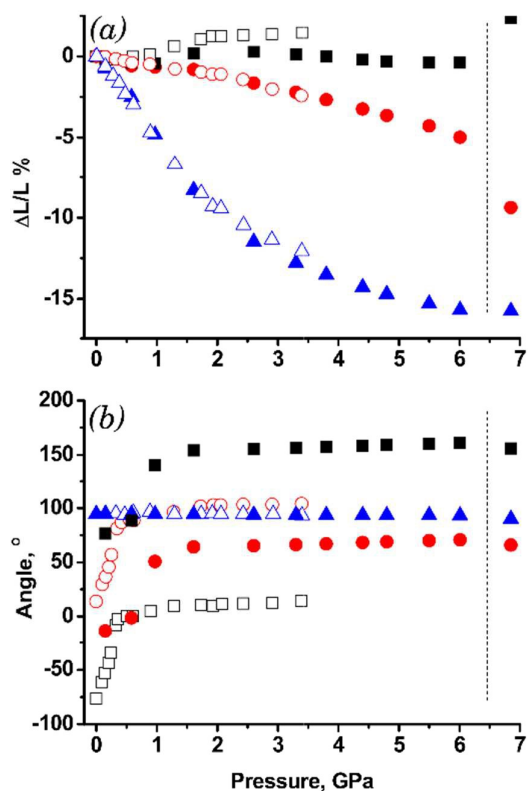


Figure 3. a) Linear strain in the directions of strain ellipsoid principal axes: squares, circles and triangles correspond to principal axes 1, 2 and 3, respectively; b) Angles between the crystallographic *a* axis and principal axis 1 (squares), the *a* axis and principal axis 2 (circles), the *a* and *c* crystallographic axes (triangles). Data measured in this work are labeled by black symbols, and selected points for $[\text{Co}(\text{NH}_3)_5\text{NO}_2]\text{Cl}_2$ taken from Ref⁹ - with open symbols.

The data on structural strain in $[\text{Co}(\text{NH}_3)_5\text{NO}_2]\text{Br}_2$ at pressures below 3.5 GPa were compared with those reported earlier for isostructural $[\text{Co}(\text{NH}_3)_5\text{NO}_2]\text{Cl}_2$ ^{9,11}. The strain anisotropy for these two compounds was similar, however not identical (Figure 3). The directions of the major compression – along the *b* axis – coincide for these systems, with minor differences in the anisotropy explained by different distributions of void space and different intermolecular interactions resulting from substitution of the Cl^- for Br^- anions. For both compounds the pressure-dependence of the *a* parameter was not monotonic, with a minimum observed below 1 GPa (Figure 1). The minimum is related to both the interchange of the medium and minor strain directions, and the different fillings of void space in the crystal structure at different pressures. For both

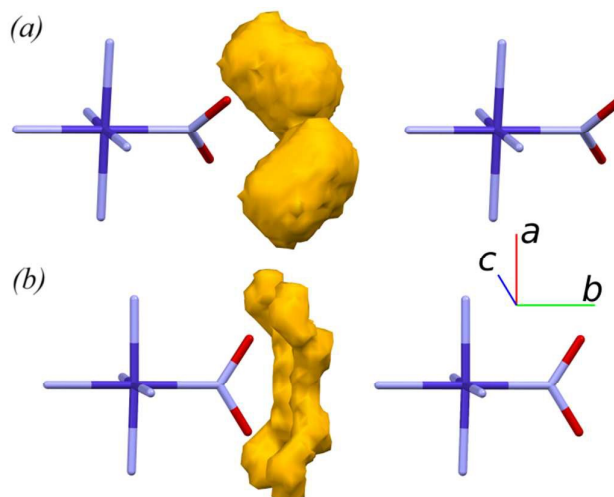


Figure 4. Voids in the crystal structure of $[\text{Co}(\text{NH}_3)_5\text{NO}_2]\text{Br}_2$ at (a) ambient pressure and (b) 6.9 GPa after the phase transition. The voids were calculated using the Mercury software²⁶ with the following parameters: (a) – contact surface, probe radius 0.8 Å, grid 0.2 Å, (b) – contact surface, probe radius 0.3 Å, grid 0.2 Å

phases the principal axes rotated at a relatively low pressure (Figure 2).

Between 6.0 and 6.9 GPa the crystal structure of $[\text{Co}(\text{NH}_3)_5\text{NO}_2]\text{Br}_2$ underwent a structural phase transition, although almost no discontinuity could be noticed on the $V(P)$ curve (Figure 1). The volume change resulting from the phase transition was $\sim -1.5\%$ (compared to -20% across the pressure range preceding the transformation). The single crystal was preserved and the space group changed from $C2/c$ to $Cmcm$. The packing of the $[\text{Co}(\text{NH}_3)_5\text{NO}_2]^{2+}$ cations and Br^- anions did not change significantly over the course of the phase transition. The main structural rearrangement was related to discontinuous rotation of the NO_2 -ligands ($\sim 31^\circ$, see animation M1 in ESI). Linear strain in the *ac* plane (in which rotation of the nitro-ligand occurs) showed discontinuities in their pressure dependences, whereas linear strain along the *b* axis was continuous. As a result of the discontinuous rotation of the NO_2 -groups, the major compression during the phase transition occurs nearly parallel to the crystallographic *c* axis. This is particularly interesting as the major compression occurs along the *b* axis prior to the phase transition. The rotation of the $-\text{NO}_2$ ligand along the Co-N bond during the phase transition is related to filling the void space in the crystal structure around this group (Figure 4).

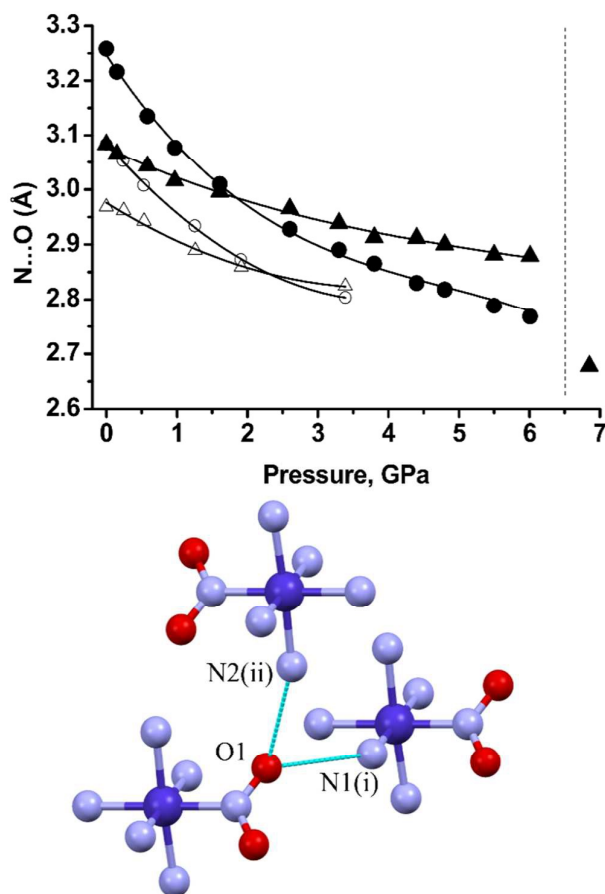


Figure 5. The changes in N1(i)...O1 (circles) and N2(ii)...O1 (triangles) distances in the hydrogen bonds on increasing pressure. Atom labeling is explained on the scheme below. Symmetry codes: (i) $1/2-x, 1/2+y, 1/2-z$, (ii) $1-y, -1/2+z$. Data measured in this work are labeled with black symbols and selected points for $[\text{Co}(\text{NH}_3)_5\text{NO}_2]\text{Cl}_2$ taken from Ref⁹ - with open symbols.

Structural studies of pressure-induced phase transitions are interesting in their own right. In the case of compounds undergoing homogeneous photo-induced reactions, accompanied by significant photomechanical effects, an additional interest exists: studying the anisotropy of interactions in the crystal. In this way one can account for the anisotropic response of a system to mechanical stresses, be this stress induced by increasing pressure or by phototransformation^{3,7}. In the case of $[\text{Co}(\text{NH}_3)_5\text{NO}_2]\text{Cl}(\text{NO}_3)$, for example, the structure showed major strain along the same crystallographic direction both on increasing pressure and in the course of photoisomerisation, but, though the change in volume was negative in both cases, linear strain along this direction was positive as a result of the reaction¹⁴ but negative on hydrostatic compression^{7,11}. This was the reason for a decreased quantum yield on external compression, despite a decrease in the molar volume that results from the reaction^{12,13}. The direction of major strain in $[\text{Co}(\text{NH}_3)_5\text{NO}_2]\text{Cl}(\text{NO}_3)$ was approximately perpendicular to the plane of NO_2 group and is related to the compression of the bands formed by hydrogen-bonded anions: NO_3^- and Cl^- ⁷.

On linkage isomerisation into the nitrito-form, the crystal structure of $[\text{Co}(\text{NH}_3)_5\text{NO}_2]\text{Br}_2$ expands significantly in direction perpendicular to the plane of NO_2 group, slightly expands along Co- NO_2 bond (b axis) and is compressed perpendicular to the plane bisecting O-N-O angle⁸. The space group changes from $C2/c$ to $Cmcm$ ⁸. These changes are very similar to the structural rearrangements that result from the pressure-induced phase transition in nitro-isomer studied in this work. Comparing the structures of the high-pressure $[\text{Co}(\text{NH}_3)_5\text{NO}_2]\text{Br}_2$ phase with that of the nitrito-form $[\text{Co}(\text{NH}_3)_5\text{ONO}]\text{Br}_2$ at ambient conditions, one can see that the nitro-group in these structures, though coordinated differently to Co, lies in the same plane with respect to the Co- NH_3 bonds in the complex cation. Compression of the structure favors rotation of the nitro-group, and this may give a clue as to the structural mechanism of linkage isomerization. The different relative compression of intermolecular N-H...O hydrogen bonds that connect the nitro-ligand to its neighbours in the crystal structure (Figure 5) is directly related to the rotation of the nitro-ligand within a complex cation, as has been previously observed in the isostructural compound, $[\text{Co}(\text{NH}_3)_5\text{NO}_2]\text{Cl}_2$ ⁹. The effect of pressure on the yield of the nitro-nitrito photoisomerisation in $[\text{Co}(\text{NH}_3)_5\text{NO}_2]\text{Br}_2$ remains unknown and deserves a dedicated study. At the same time, it has already been shown that increasing pressure speeds up the nitrito-nitro thermoisomerization, $[\text{Co}(\text{NH}_3)_5\text{ONO}]\text{Br}_2 \rightarrow [\text{Co}(\text{NH}_3)_5\text{NO}_2]\text{Br}_2$ ^{31,32}.

Conclusions

Structural changes in $[\text{Co}(\text{NH}_3)_5\text{NO}_2]\text{Br}_2$ on increasing pressure were shown to be related to the strain that results from the solid-state linkage isomerization, involving the rotation of the nitro-group. Thus the mechanism of a pressure-induced phase transition can shed light on the structural mechanism of this intramolecular solid-state reaction. One can rationalise the previously measured effect of pressure on the rate of thermal isomerisation in $[\text{Co}(\text{NH}_3)_5\text{ONO}]\text{Br}_2$ ³² and expect that pressure should also have a pronounced effect on the yield of the linkage photoisomerisation in $[\text{Co}(\text{NH}_3)_5\text{NO}_2]\text{Br}_2$. This hypothesis can be tested by an *in situ* single-crystal diffraction study at high pressure and deserves a dedicated study, similar to recently documented works^{33,34}.

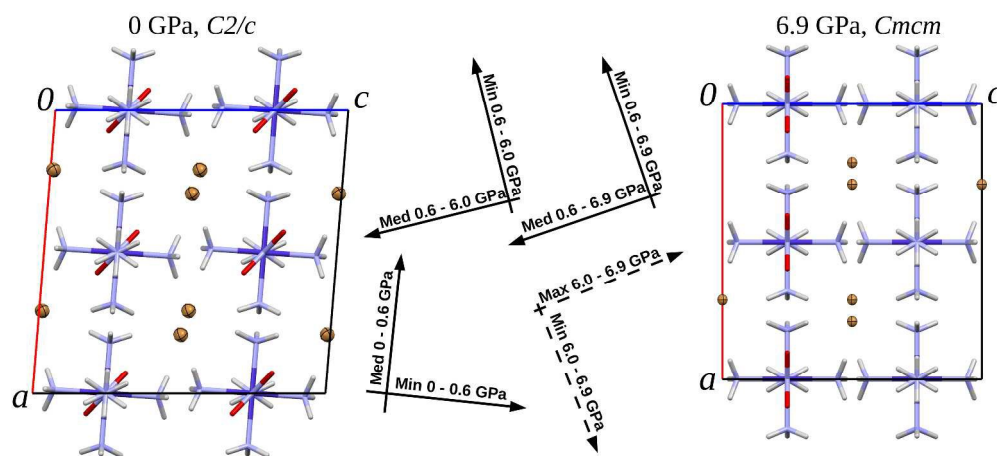
Acknowledgements

The work was supported by the Ministry of Education and Science of the Russian Federation (project 1828), Russian Academy of Sciences and a RFBR project 14-03-00902.

Notes and references

- 1 A. P. Chupakhin, A. A. Sidel'nikov and V. V. Boldyrev, *React. Solids*, **3**, 1–19.
- 2 E. V. Boldyreva and V. V. Boldyrev, Eds., *Reactivity of Molecular Solids*, Wiley: Chester, 1999, and references therein.
- 3 P. Naumov, S. Chizhik, M. Panda, N. Nath and E. Boldyreva, *Chem. Rev.*, 2015, accepted, and references therein.

- 4 E. V. Boldyreva, A. A. Sidelnikov, A. P. Chupakhin, N. Z. Lyakhov and V. V. Boldyrev, E.V. Boldyreva, A.A. Sidelnikov, A.P. Chupakhin, N.Z. Lyakhov, V.V. Boldyrev, *Doklady Phys. Chem.* [Doklady Akademii Nauk SSSR Phys. Chem.], 1984, **277**, 893-896; CA 1984:619590.
- 5 E. Boldyreva, *Mol. Cryst. Liq. Cryst. Inc. Non-Lin. Opt*, 1994, **242**, 17-52.
- 6 E. V. Boldyreva, *Russ. J. Coord. Chem.* [Koord. Khim.], 2001, **27**, 297-323, and references therein.
- 7 P. Naumov, S. C. Sahoo, B. A. Zakharov and E. V Boldyreva, *Angew. Chem. Int. Ed. Engl.*, 2013, **52**, 9990-9995.
- 8 N. Masciocchi, A. Kolyshev, V. Dulepov, E. Boldyreva and A. Sironi, *Inorg. Chem.*, 1994, **33**, 2579-2585.
- 9 E. V. Boldyreva, D. Y. Naumov and H. Ahsbahs, *Acta Crystallogr. B*, 1998, **54**, 798-808.
- 10 E. Boldyreva, In: *High-Pressure Crystallography. From Novel Experimental Approaches to Applications in Cutting-Edge Technologies* (Eds. E. Boldyreva, P. Dera), Springer: Dordrecht, 2010, 147-159.
- 11 E. V. Boldyreva, H. Ahsbahs and H. Uchtmann, *Ber. Bunsen. Phys. Chem.*, 1994, **98**, 738-745.
- 12 E. V. Boldyreva and A. A. Sidelnikov, *Izv. Sib. Otd. Akad. Nauk SSSR, Ser. Khim. Nauk*, 1987, **5**, 139-145.
- 13 B. I. Yakobson, E. V. Boldyreva and A. A. Sidelnikov, *Izv. Sib. Otd. Akad. Nauk SSSR, Ser. Khim. Nauk*, 1989, **1**, 6-10.
- 14 E. V. Boldyreva, A. V. Virovets, L. P. Burleva, V. E. Dulepov and N. V. Podberezskaya, *J. Struct. Chem.* [Zhurnal Strukt. Khimii], 1993, **34**, 128-140.
- 15 R. Boehler, *Rev. Sci. Instrum.*, 2006, **77**, 115103-1-115103-3.
- 16 G. J. Piermarini, *J. Appl. Phys.*, 1973, **44**, 5377-5382.
- 17 R. J. Angel, M. Bujak, J. Zhao, G. D. Gatta and S. D. Jacobsen, *J. Appl. Crystallogr.*, 2007, **40**, 26-32.
- 18 G. J. Piermarini, S. Block, J. D. Barnett and R. A. Forman, *J. Appl. Phys.*, 1975, **46**, 2774-2780.
- 19 CrysAlisPro. Agilent Technologies UK, Yarnton, Oxfordshire, UK, 2013.
- 20 R. Angel and J. Gonzalez-Platas, *J. Appl. Crystallogr.*, 2013, **46**, 252-254.
- 21 E. V. Boldyreva, J. Kivikoski and J. A. K. Howard, *Acta Crystallogr. Sect. C Cryst. Struct. Commun.*, 1997, **53**, 523-526.
- 22 G. M. Sheldrick, *Acta Crystallogr. Sect. C Struct. Chem.*, 2015, **71**, 3-8.
- 23 X-STEP. Stoe&Cie, Darmstadt, Germany, 2000.
- 24 R. J. Angel, *Win_Strain*, 2011, www.rossangel.com.
- 25 M. C. Burla, R. Caliendo, M. Camalli, B. Carrozzini, G. L. Cascarano, L. De Caro, C. Giacovazzo, G. Polidori and R. Spagna, *J. Appl. Crystallogr.*, 2005, **38**, 381-388.
- 26 C. F. Macrae, P. R. Edgington, P. McCabe, E. Pidcock, G. P. Shields, R. Taylor, M. Towler and J. van de Streek, *J. Appl. Crystallogr.*, 2006, **39**, 453-457.
- 27 A. L. Spek, *Acta Crystallogr. D. Biol. Crystallogr.*, 2009, **65**, 148-155.
- 28 F. H. Allen, O. Johnson, G. P. Shields, B. R. Smith and M. Towler, *J. Appl. Crystallogr.*, 2004, **37**, 335-338.
- 29 F. H. Allen, *Acta Crystallogr. Sect. B Struct. Sci.*, 2002, **58**, 380-388.
- 30 E. Boldyreva, J. Kivikoski and J. A. K. Howard, *Acta Crystallogr. Sect. B Struct. Sci.*, 1997, **53**, 405-414.
- 31 E. V. Boldyreva, S. L. Kuzmina and H. Ahsbahs, *J. Struct. Chem.*, **39**, 343-349.
- 32 E. V. Boldyreva, S. L. Kuzmina and H. Ahsbahs, *J. Struct. Chem.*, 1998, **39**, 762-773.
- 33 J. Bąkiewicz and I. Turowska-Tyrk, *J. Photochem. Photobiol. A: Chem.*, 2012, **232**, 41-43.
- 34 J. Bąkiewicz and I. Turowska-Tyrk, *CrystEngComm*, 2014, **16**, 6039-6048.
- 35 K. Konieczny, J. Bąkiewicz and I. Turowska-Tyrk, *CrystEngComm*, 2015, **17**, 7693-7701.



A single-crystal to single-crystal phase transition above 6.0 GPa is discussed in relation to the structural mechanism of homogeneous linkage photoisomerisation that is accompanied by photomechanical effects in the same compound.

1185x535mm (96 x 96 DPI)